Hierarchical architectures by synergy between dynamical template self-assembly and biomineralization

EMILIE POUGET[1], ERIK DUJARDIN[2], ANNIE CAVALIER[3], ALAIN MOREAC[1], CÉLINE VALÉRY[4], VALÉRIE MARCHI-ARTZNER[5], THOMAS WEISS[6], ANNE RENAULT[1], MAITÉ PATERNOSTRE[7] AND FRANCK ARTZNER[1]*

[1]Groupe Matière Condensée et Matériaux, UMR 6626 CNRS et Université Rennes 1, 263 Avenue du général Leclerc, 35042 Rennes Cedex, France
[2]NanoSciences Group, CEMES UPR 8011 CNRS, BP 94347, 29 r. J. Marvig, 31055 Toulouse Cedex 4, France
[3]Interactions Cellulaires et Moléculaires, UMR 6026 CNRS et Université Rennes 1, 263 Avenue du général Leclerc, 35042 Rennes Cedex, France
[4]Ipsen Pharma S.A., Ctra. Laurea Miro 395, 08980-Sant Feliu de Llobregat, Barcelona, Spain
[5]Sciences Chimiques de Rennes, UMR 6226 CNRS et Université Rennes 1, 263 Avenue du général Leclerc, 35042 Rennes Cedex, France
[6]ESRF, 6 rue Jules Horowitz, BP220, 38043 Grenoble Cedex, France
[7]URA 2096, IBiTechS, CEA-Saclay, F-91191 Gif/Yvette, France
*e-mail: franck.artzner@univ-rennes1.fr

Published online: 21 May 2007; doi:10.1038/nmat1912

Diatoms, shells, bones and teeth are exquisite examples of well-defined structures, arranged from nanometre to macroscopic length scale, produced by natural biomineralization using organic templates to control the growth of the inorganic phase[1–6]. Although strategies mimicking Nature have partially succeeded in synthesizing human-designed bio-inorganic composite materials[7–10], our limited understanding of fundamental mechanisms has so far kept the level of hierarchical complexity found in biological organisms out of the chemists' reach[11]. In this letter, we report on the synthesis of unprecedented double-walled silica nanotubes with monodisperse diameters that self-organize into highly ordered centimetre-sized fibres. A unique synergistic growth mechanism is elucidated by the combination of light and electron microscopy, synchrotron X-ray diffuse scattering and Raman spectroscopy. Following this growth mechanism, macroscopic bundles of nanotubules result from the kinetic cross-coupling of two molecular processes: a dynamical supramolecular self-assembly and a stabilizing silica mineralization. The feedback actions between the template growth and the inorganic deposition are driven by a mutual electrostatic neutralization. This 'dynamical template' concept can be further generalized as a rational preparation scheme for materials with well-defined multiscale architectures and also as a fundamental mechanism for growth processes in biological systems.

The growth and form of natural biomaterials have been a long-standing subject of questioning by biologists and also by materials scientists, as, beyond complex morphologies, natural hierarchical materials usually possess remarkably optimized properties such as mechanical stiffness[5,12], light conduction[2,4,6] or even multifunctions on multiple length scales. Inspired by these natural templates, we wish to be able to mimic them for human-designed applications in nanomaterials science[4] and biotechnology[11], for example. Unfortunately, the rational synthesis of complex forms still lacks flexibility, primarily because underlying growth mechanisms remain largely hypothetical for both natural and biomimetic structures[13–16]. In this regard, a better understanding of molecular mechanisms controlling the morphogenesis of bio-inorganic composite materials would foster a more efficient design of simplified models of natural nanostructured biomaterials[8,11,17]. For instance, there is a current consensus that biotemplated silica materials are produced from the interaction of silica precursors with self-assembling proteins containing amine moieties[13,14,18,19]. However, whether the organic matrix is preformed or dynamically grown under the influence of the mineralization is still open. In this work, we investigate the bio-inspired silica mineralization processes of well-characterized self-assembled peptide structures. Indeed, we have recently shown that lanreotide, a dicationic octapeptide (Fig. 1a), self-assembles in pure water into nanotubes with a monodisperse diameter of 24.4 nm and a wall thickness of 1.8 nm, the structure of which has been resolved at supramolecular as well as molecular levels[20,21]. In particular, the presence of two exposed protonable amine groups per octapeptide makes the lanreotide nanotubes a potential template for silica growth as presented hereafter[14–16].

The mineralization of these precisely designed tubes is obtained by bringing into contact a lanreotide gel and a tetraethylorthosilicate (TEOS) solution in water within the confined volume of 1.5-mm-diameter glass capillaries (Fig. 1b). Initially, a turbid gel of lanreotide nanotubes is set at the bottom of the capillary and a TEOS/water mixture is added (Fig. 1b, tube 1). Following a slow kinetics, a clear phase appears in the upper part of the lanreotide zone (region 1), while the turbid phase recedes. The small-angle X-ray scattering (SAXS) of the clear section in region 1 indicates that the lanreotide nanotubes are dissociated and that a dilute aqueous solution of the peptide with a concentration lower than 2.5% (w/w) is produced. After few days, centimetre-long white fibres are formed in the TEOS solution (Fig. 1b, tubes 3 and 4,

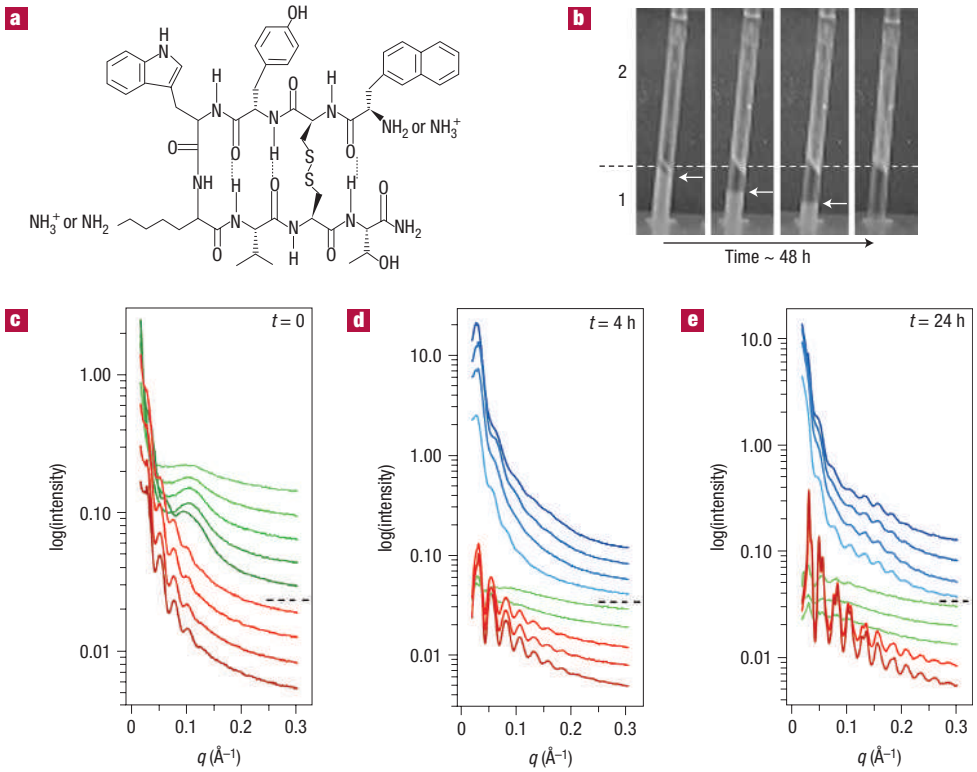

Figure 1 Silica mineralization of lanreotide. **a**, Structure of the lanreotide octapeptide showing the two charged amine sites. **b**, Time-lapsed pictures of the capillaries during the mineralization process. Initially, a volume of lanreotide gel at 5% (w/w) poured into the bottom of the capillary (region 1) is covered with the same volume of a 30% (w/w) TEOS/water mixture (region 2) (tube 1). On ageing, the lanreotide turbid gel recedes (white arrows), yielding a transparent region, while long white fibres appear in region 2, starting from the interface (tubes 2 and 3). After 48 h, the lanreotide gel has completely disappeared and only two phases separated by a white ring are observed: the lower clear one containing a dilute lanreotide solution and the upper one filled with mineralized fibres (tube 4). **c–e**, SAXS diffraction patterns taken at $t = 0$ (**c**), $t = 4$ h (**d**) and $t = 24$ h (**e**), at regular intervals along capillaries on either side of the interface represented by the horizontal dotted lines. Spectra have been shifted along the *y*-axis for clarity. The lanreotide gel (red) and the lanreotide solutions (green) show characteristic spectra[21]. A new phase (blue) is observed in region 2 after 24 h.

region 2), which have been extensively characterized by a panel of techniques in three sequential states: (1) fibres in their growth solution; (2) dried fibres prepared by repeated water washing and drying; (3) replicas obtained by calcination at 600 °C. Surprisingly, no mineralization is observed in the lanreotide gel or in the clear solution of region 1. Transmission electron microscopy (TEM) on dried fibres and replicas reveals that they are constituted by bundles of aligned inorganic nanotubes with homogeneous inner and outer diameters of 15 ± 1 nm and 29 ± 2 nm respectively (Fig. 2a,b). Higher-magnification micrographs (Fig. 3a,b) show that the nanotube walls are composed of three concentric layers that are successively high, low and high in electron density, suggesting a coaxial structure with a double-walled silica tube coating the inner and outer surfaces of the organic template. Figure 3c,d shows perfectly reproducible SAXS clichés recorded at various locations along a fibre axis and for about 100 samples. Such SAXS clichés confirm the very homogeneous structure of the hybrid silica–lanreotide nanotubes. Indeed, more than 12 short oscillations are observable thanks to the monodispersity of the cylindrical shape. Moreover, the cosine envelope (Fig. 3d, red dotted line) is a signature of the double wall with a well defined distance between the inner and outer silica deposits. The simulation of the SAXS spectra (see the Methods section) yields a mean diameter of 24.6 nm, internal and external silica walls of identical 1.4 nm thickness and a lanreotide template thickness of 2 nm, in good agreement with TEM data (Fig. 3e). Furthermore, the molecular organization of the organic template between the two silica walls is preserved during the mineralization, as shown by Raman spectra (see Supplementary Information, Fig. S1) and by X-ray diffraction with the presence of the 0.35 $Å^{-1}$ peak (green arrow in Fig. 3c), characteristic of the β-sheet organization in the lanreotide wall surface[20]. A final calcination step at 600 °C converts hybrid organic–inorganic nanostructures into pure silica double-walled nanotubes (see Supplementary Information, Fig. S2). Beyond the molecular self-assembly and the nanoscale tubular structures, the templated mineralization of lanreotide results in higher-order architectures at the micro- and macroscale. Electron micrographs show that individual nanotubes reach 1–3 μm in length and bundles of closely packed aligned nanotubes are observed to exceed 7 μm (Fig. 2b). The macroscale organization is reflected in the optical properties of all three sequential states of the fibres. In particular, the strong birefringence (Fig. 2c) and its extinction (Fig. 2d) observed in polarized light microscopy for polarizers parallel to the fibre main axis demonstrate that the fibres consist of anisotropic entities ordered along a common orientation throughout the length scales from one micron to one centimetre (Fig. 2e and see Supplementary Information, Fig. S3). Hence, the structural hierarchical characteristics of the silica-mineralized lanreotide fibres span more than six orders of magnitude from the precisely controlled growth of the inorganic phase on the template at the molecular level to the ordered organization of nanoscale objects up to the macroscopic level.

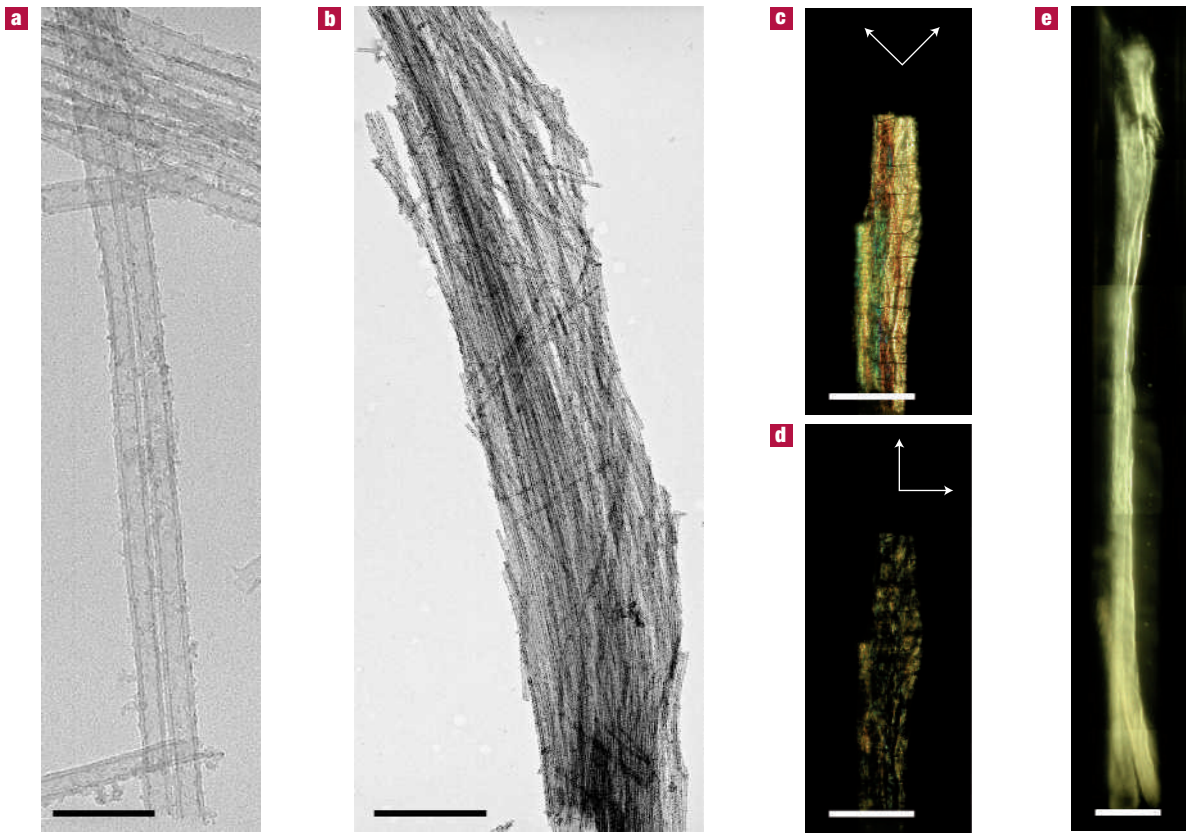

Figure 2 Multiscale organization of silica–lanreotide nanotubes. a, Transmission electron micrograph of double-walled silica nanotube replica after calcination. **b**, Transmission electron micrograph of a 7-μm-long bundle of dried mineralized nanotubes. **c**,**d**, High- and **e**, low-magnification cross-polarized optical microscopy images of a centimetre-long dried hybrid fibre (white arrows indicate the light polarization). Extinction is observed only when the light is polarized along the fibre axis (**d**), revealing the uniaxial orientation of the nanotubes within the fibre, whereas bright birefringence is recorded when light is polarized at 45° (**c**,**e**). Scale bars are **a**, 100 nm; **b**, 1 μm; **c**,**d**, 200 μm; **e**, 1 mm.

Interestingly, notwithstanding the clearly templated growth process, several experimental observations indicate that direct mineralization of preformed lanreotide nanotubes cannot explain the observed superstructures. As already underlined, the hybrid-nanotube growth does not occur in the lanreotide gel phase but in the upper aqueous TEOS solution at the same time as the gel is consumed (Fig. 1b). Indeed, SAXS spectra acquired at regular intervals along the capillary at different stages in the mineralization process are presented in Fig. 1c–e. Immediately after bringing the reactant into contact, region 1 yields only lanreotide nanotube spectra (red curves)[20], whereas region 2 is characterized by diffuse scattering due to lanreotide solution[21], the concentration of which is decreasing as a function of distance from the interface (Fig. 1c, green curves). Consequently, preformed nanotubes do not exist in region 2 before silica condensation. Furthermore, after a few hours, initial nanotubes in region 1 are unaffected, and the intensity of the central diffusion signal increases in region 2 significantly as TEOS starts to condense into silica (Fig. 1d, blue curves). After 24 h, region 1 still shows receding nanotube-gel and expanding clear-solution phases. Noticeably, spectra of silica-coated nanotubes appear in region 2 (Fig. 1e, blue curves). Second, TEM observations show that the thicknesses of inner and outer silica walls are strictly identical (1.4 nm) and homogeneous along the entire tube length for all observed nanotubes (Figs 2a and 3). This can hardly be accounted for by the identical diffusion of silica precursors into and onto preformed nanotube templates, because diffusion-limited transport of silica reactant inside the narrow nanotube cavity would result in a dissymmetry between the inner and outer wall thicknesses. On the contrary, because the organic gel is in a dynamic equilibrium with free lanreotide[21], it acts as a reservoir, providing free octapeptide, which diffuses into the hydrolysed TEOS solution, where it reforms nanotubes in the presence of reactive silica species. Moreover, such a dynamic templating mechanism does not restrict the morphology of the replica to the initial nanotube size, nor does it limit the diffusion of reactant inside the nanotubes. Therefore, centimetre-long mineralized fibres can grow from the template that is formed *in situ* under the guidance of the self-assembly process. Although dynamical templating is widespread in supramolecular self-organization processes[22], it has been proposed for hybrid organic/inorganic mesoporous silica formation only recently[23].

Our proposed dynamic templating mechanism accounts for two distinct self-assembly processes occurring simultaneously: the nanotube organic template formation and the silica polymerization. The regularity of the composite wall structure strongly supports the idea that the two processes are intimately entangled (Fig. 4). This coupling necessarily occurs at the extremity of the template, where it self-assembles, at the same time that the silica precursors are condensing. In this scenario, both inner and outer silica walls are equivalently accessible for the silica precursor by diffusion to the tip of the growing hybrid nanotube. The coupling of two molecular processes requires a mutual

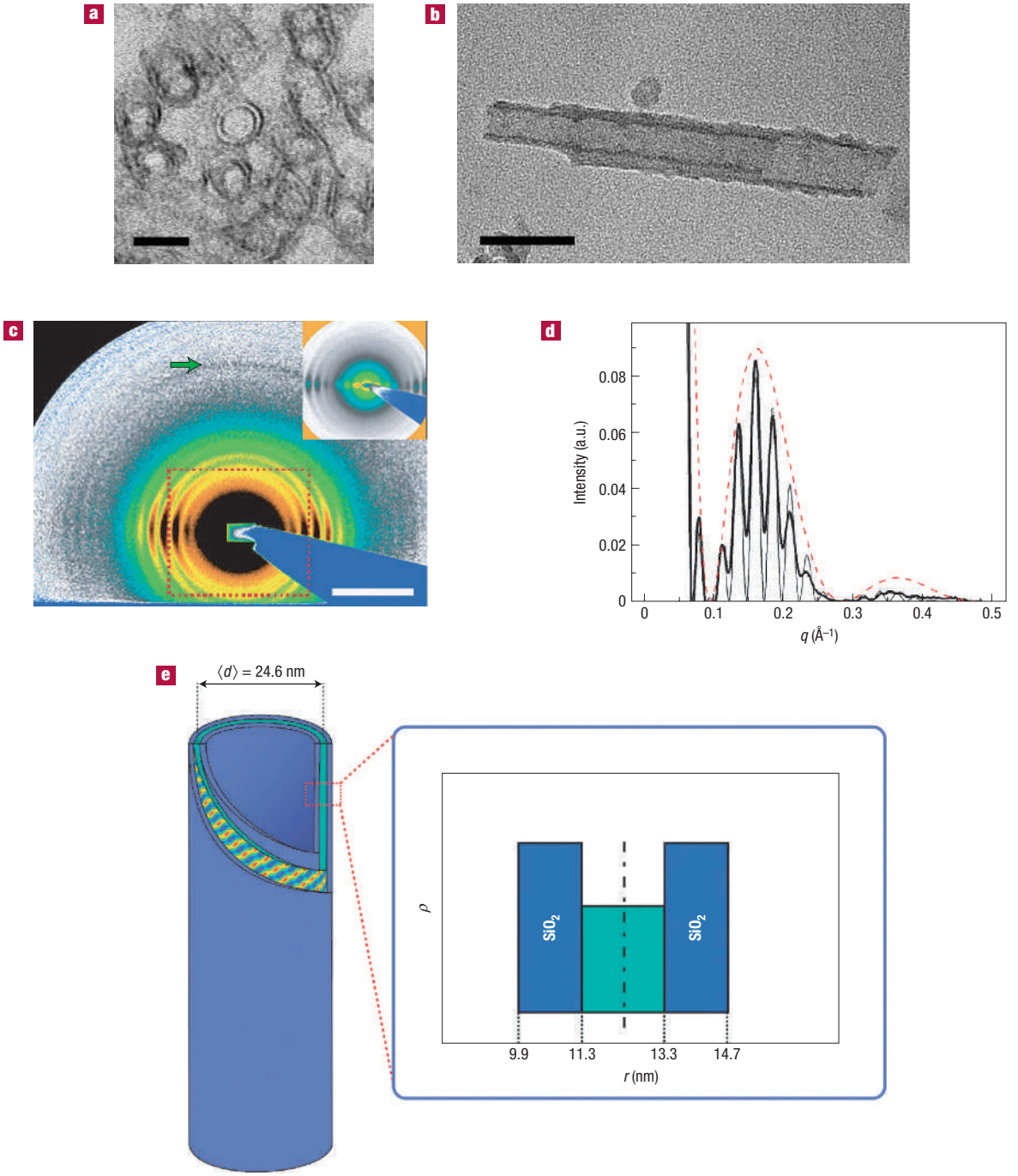

Figure 3 Evidence for double-walled silica–lanreotide nanotubes. a, Cross-sectional TEM image of dried fibres, revealing several concentric circles due to the double-wall structure. **b**, TEM image of a fragment of dried nanotube, showing that the internal and external cylinders are independent and free to slide. **c**, SAXS clichés of an as-synthesized fibre with a sample–detector distance of 1.2 m (inset: 3 m). **d**, SAXS diffraction pattern (bold black line). The peak envelope (form factor, red dotted line) is clearly observed, with well-resolved individual peaks that can be adjusted to the fitting model (fine black line). **e**, Schematic representation of a silica–lanreotide nanotube with an inner and an outer 1.4-nm-thick silica shell (blue) and a central 2.0-nm-thick lanreotide tube (green) as deduced from radial density (ρ) profiles. Scale bars are **a**, 30 nm; **b**, 50 nm; **c**, 0.2 $Å^{-1}$.

feedback, which implies two regulation mechanisms between silica condensation (Fig. 4, step C) and template self-assembly (Fig. 4, step T_{on}). First, controlled experiments with diluted solutions of lanreotide showed that the sole presence of the lanreotide is insufficient to initiate the silica condensation. We postulate that Coulomb interactions between the positively charged lanreotide nanotube surface and the slightly negatively charged silica precursors are driving the cooperative processes. Indeed, we have recently shown that the pure lanreotide self-assembly into nanotubes in water is driven by hydrophobic interactions but is hampered by the electrostatic repulsion between free cationic lanreotide molecules and charged nanotubes[20]. This

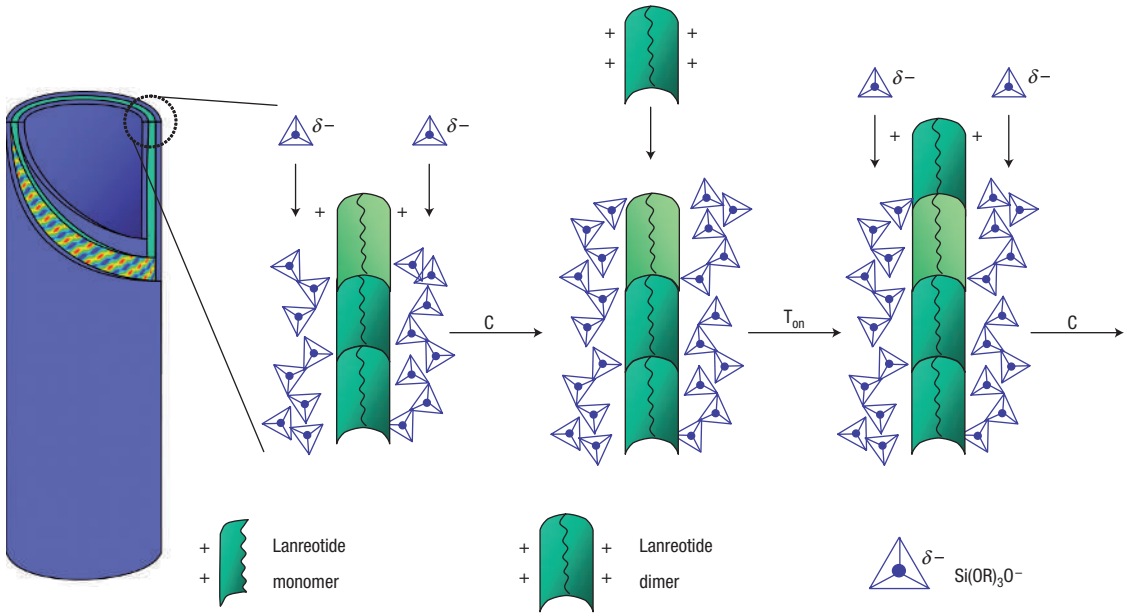

Figure 4 Dynamic template model for the growth mechanism of the peptide–silica fibres. The cationic lanreotide nanotube surface catalyses the silica condensation by electrostatic forces (step C) and the anionic silica deposit promotes the lanreotide assembly (step T_{on}) by synergetic neutralization of the system.

repulsion vanishes with the neutralization by the silica deposition, which promotes the nanotube growth although the monomer concentration is low. The application of the Gouy–Chapman theory[24] shows that the concentration of silica precursor R_3SiO^- in the vicinity of the positively charged lanreotide surface is 30 times higher than in the bulk solution. This ensures the spatial selectivity of the template surface and locally accelerates the silica condensation (Fig. 4, step C). The mineralization reaction generally leads to a slightly negatively charged silica deposit due to unreacted silanol groups[25]. In the present system, the silica coating compensates for the cationic template charge until neutralization of the hybrid nanotube is reached for a well-defined deposit thickness, preventing further catalysis of the condensation. Indeed, a complete consumption of the reactants cannot be invoked, because the TEOS solution is still rich in reactive hydrolysed silica species after synthesis, as seen by the instantaneous precipitation induced by the addition of 0.5 M sodium hydroxide to the solution.

Neutralization of Coulomb interactions is therefore the underlying principle governing synergistically the surface-confined condensation of silica into tubes of uniform thickness and the growth of extended unidimensional tubular peptidic templates. On the one hand, the silica polymerization is activated by the slight excess of peptides during the template growth. On the other hand, the octapeptide assembly/de-assembly equilibrium is shifted towards the formation of long nanotubes by the continuous neutralization of the reformed template. Conversely, silica deposition is inhibited where the template is lacking and peptide self-assembly in the reaction medium is negligible in the absence of silica condensation. In summary, the local coupling of the self-assembly processes derives from two cross-linked feedback mechanisms at the molecular scale, both involving Coulomb interactions between the two oppositely charged building blocks, namely silicates and lanreotide peptides.

In this letter, we demonstrate that the kinetic coupling of two fundamental mineralization mechanisms produces unique synthetic organic–inorganic materials with hierarchical features spanning more than six orders of magnitude. In previous works, the morphological control was restricted to either nanoscopic features such as double walls[26] and wall thickness[27] or the macroscopic length[28]. Significantly, in the proposed coupling mechanism, the spatio-temporal coordination regulates recursively the template self-assembly and its coating, and thus results in higher-order macroscopic constructions with nanometric precision. At the same time, the dynamical template offers the unique opportunity to generate architectures far beyond the initial size of the template.

Although the complexity of biological systems is not achieved in the reported case, it also provides a further insight into fundamental mechanisms possibly occurring in biological hierarchical architectures. For instance, biosilica formation has been related to the higher reactivity of silica precursors with silaffin[14] or silicatein[13,18] in their template self-assembled forms rather than with their soluble forms, in agreement with the exaltation of the Coulomb interactions close to charged surfaces described above. Another open question is the formation mechanism of spicules of desmosponges, which can reach macroscopic length[2,29,30]. Here also, the classical static template mechanism has been excluded, whereas the dynamical template emerges as an explanation compatible with such biomineralized architectures larger than biological templates[18,19]. Pursuing such a dialectic between better described morphogenesis of natural architectures and refined synthetic model systems will doubtlessly open countless possibilities to design and produce more sophisticated functional materials for biological and technological applications.

METHODS

MATERIALS

Cyclic lanreotide (sequence NH_2–(D)Naph-Cys–Tyr–(D)Trp–Lys–Val–Cys–Thr–$CONH_2$; BIM 23014C) was obtained from Ipsen Pharma (Barcelona) as an acetate salt (molecular masses of 1,095 Da, purity >98%). Mixtures were made by dissolving the peptide powders at 5% w/w in pure water. TEOS (purity > 99%) was purchased from Sigma and used as received.

SYNTHESIS

Lanreotide nanotube gels were prepared at ambient temperature using lanreotide acetate powder dissolved in pure water (5% w/w). The silica precursor solution is an emulsion of TEOS in water (30% w/w), prepared 24 h before use. The fibre syntheses were carried out in 1.5 mm glass capillaries (GLAS Technik & Konstruktion). The samples were prepared by sequential deposition of first 15 µl of lanreotide gel and then 15 µl of the silica precursor in the capillary. The fibres appeared after a time ranging from 48 h to one week. The resulting white fibres were removed from the tube and dried under vacuum at 80 °C. Inorganic replicas were obtained by calcination of the peptide by heating up to 600 °C.

OPTICAL MICROSCOPY

The samples were observed directly in the capillaries or on a glass slide with an Olympus IX70 microscope equipped with two crossed polarizers.

ELECTRON MICROSCOPY

Fibres were dispersed in ethanol by sonication for 3 min and drop-casting onto carbon-coated copper EM grids. For cross-sectional imaging, the fibres were rinsed with water, followed by dehydration in 90% ethanol, and embedded in an Epon-Araldite mixture. Ultra-thin sections obtained by ultramicrotomy were collected onto copper grids. Observations were carried out on Philips CM12 microscopes operated at 100 kV.

SAXS

X-ray diffraction experiments were carried out at the High Brilliance beamline (ID2), European Synchrotron Radiation Facility in Grenoble, France. The beam size defined by the collimating slits was 0.2 mm × 0.2 mm. The detector was an image-intensified CCD (charge-coupled device) camera, and the sample-to-detector distance varied between 120 and 300 cm.

SAXS SIMULATION

The intensity of the radial integration of this SAXS can be simulated by order-one Bessel functions, J_1, corresponding to the Fourier transform of a multilayer tube:

$$I(q) = \left(\frac{\delta_1 r_1 J_1(r_1 q) + \delta_2 r_2 J_1(r_2 q) - \delta_2 r_3 J_1(r_3 q) - \delta_1 r_4 J_1(r_4 q)}{q} \right)^2$$

where r_1, r_2, r_3 and r_4 correspond to the cylinder radius, r_1 and r_2 being respectively the internal and external diameter of the internal silica cylinder, and r_3 and r_4 being respectively the internal and external diameter of the external silica cylinder. δ_1 and δ_2 are the differences of the electron density between water and silica or silica and lanreotide respectively.

COULOMB ATTRACTION BY A CHARGED SURFACE

For a surface composed of cationic molecules, the Gouy–Chapman theory[24] predicts that anions A^- are attracted by the positive surface with a concentration increase of $[A^-]_0/[A^-]_\infty = \exp[(-ze\psi_0)/kT]$, where e is the electron charge, z the charge of the ion, $z = 2$, and ψ_0 the electrostatic potential, $\psi_0 = 93$ mV when $3.0 < \mathrm{pH} < 6.5$. The theoretical excess of anions in the neighbouring surface on increasing the solution pH is shown in Supplementary Information, Fig. S4.

Received 22 December 2006; accepted 30 March 2007; published 21 May 2007.

References

1. Lowenstam, H. A. & Weiner, S. *On Biomineralisation* (Oxford Univ. Press, New York, 1989).
2. Sundar, V. C., Yablon, A. D., Grazul, J. L., Ilan, M. & Aizenberg, J. Fibre-optical features of a glass sponge. *Nature* **424**, 899–900 (2003).
3. Politi, Y., Arad, T., Klein, E., Weiner, S. & Addadi, L. Sea urchin spine calcite forms via a transient amorphous calcium carbonate phase. *Science* **306**, 1161–1164 (2004).
4. Aizenberg, J. & Hendlen, G. Designing efficient microlens arrays: Lessons from Nature. *J. Mater. Chem.* **14**, 2066–2072 (2004).
5. Aizenberg, J. *et al.* Skeleton of Euplectella sp.: Structural hierarchy from the nanoscale to the macroscale. *Science* **309**, 275–278 (2005).
6. Aizenberg, J., Sundar, V. C., Yablon, A. D., Weaver, J. C. & Chen, G. Biological glass fibers: Correlation between optical and structural properties. *Proc. Natl Acad. Sci. USA* **101**, 3358–3363 (2004).
7. Mann, S. *Biomineralization. Principles and Concepts in Bioinorganic Materials Chemistry* (Oxford Univ. Press, Oxford, 2001).
8. Dujardin, E. & Mann, S. Bio-inspired materials chemistry. *Adv. Mater.* **14**, 775–788 (2002).
9. Yang, H., Coombs, N. & Ozin, G. A. Morphogenesis of shapes and surface patterns in mesoporous silica. *Nature* **386**, 692–695 (1997).
10. Hartgerink, J. D., Beniash, E. & Stupp, S. I. Self-assembly and mineralization of peptide–amphiphile nanofibers. *Science* **294**, 1684–1688 (2001).
11. Sanchez, C., Arribat, H. & Giraud-Guille, M. M. Biomimetism and bioinspiration as tools for the design of innovative materials systems. *Nature Mater.* **4**, 277–288 (2005).
12. Woesz, A. *et al.* Micromechanical properties of biological silica skeletons of deep-sea sponges. *J. Mater. Res.* **21**, 2068–2078 (2006).
13. Cha, J. N. *et al.* Silicatein filaments and subunits from a marine sponge direct the polymerization of silica and silicones in vitro. *Proc. Natl Acad. Sci. USA* **96**, 361–365 (1999).
14. Kröger, N., Lorenz, S., Brunner, E. & Sumper, M. Self-assembly of highly phosphorylated silaffins and their function in biosilica morphogenesis. *Science* **298**, 584–586 (2002).
15. Hukkamaki, J. & Pakkanen, T. T. Amorphous silica materials prepared by neutral templating route using amine-terminated templates. *Micro. Meso. Mater.* **65**, 189–196 (2003).
16. Van Bommel, K. J. C. & Shinkai, S. Silica transcription in the absence of a solution catalyst: The surface mechanism. *Langmuir* **18**, 4544–4548 (2002).
17. Shimizu, T., Masuda, M. & Minamikawa, H. Supramolecular nanotube architectures based on amphiphilic molecules. *Chem. Rev.* **105**, 1401–1443 (2005).
18. Schroder, H. C. *et al.* Co-expression and functional interaction of silicatein with galectin—Matrix-guided formation of siliceous spicules in the marine demosponge *Suberites domuncula*. *J. Biol. Chem.* **281**, 12001–12009 (2006).
19. Schroder, H. C. *et al.* Apposition of silica lamellae during growth of spicules in the demosponge *Suberites domuncula*: Biological/biochemical studies and chemical/biomimetical confirmation. *J. Struct. Biol.* (in the press).
20. Valéry, C. *et al.* Biomimetic organization: Octapeptide self-assembly into nanotubes of viral capsid-like dimension. *Proc. Natl Acad. Sci. USA* **100**, 10258 (2003).
21. Valéry, C. *et al.* Self-association process of a peptide in solution: From beta-sheet filaments to large embedded nanotubes. *Biophys. J.* **86**, 2484 (2004).
22. Lehn, J.-M. *Supramolecular Chemistry: Concepts and Perspectives* (VCH, Weinheim, 1995).
23. Lesaint, C., Lebeau, B., Marichal, C., Patarin, J. & Zana, R. Fluorescence probing investigation of the mechanism of formation of MSU-type mesoporous silica prepared in fluoride medium. *Langmuir* **21**, 8923–8929 (2005).
24. Israelachvili, J. *Intramolecular and Surface Forces* 2nd edn (Academic, San Diego, 1992).
25. Brinker, C. J. & Scherer, G. W. *Sol–Gel Science. The Physics and Chemistry of Sol–Gel Processing* (Academic, New York, 1990).
26. Ji, Q. *et al.* Direct sol–gel replication without catalyst in an aqueous gel system: From a lipid nanotube with a single bilayer wall to a uniform silica hollow cylinder with an ultrathin wall. *Chem. Mater.* **16**, 250–254 (2004).
27. Ji, Q., Iwaura, R. & Shimizu, T. Controlling wall thickness of silica nanotubes within 4-nm precision. *Chem. Lett.* **33**, 504–505 (2004).
28. Adachi, M., Harada, T. & Harada, M. Formation of huge length silica nanotubes by a templating mechanism in the laurylamine/tetraethoxysilane system. *Langmuir* **15**, 7097–7100 (1999).
29. Uriz, M. J., Turon, X., Becerro, M. A. & Agell, G. Siliceous spicules and skeleton frameworks in sponges: Origin, diversity, ultrastructural patterns and biological functions. *Microsc. Res. Technol.* **62**, 279–299 (2003).
30. Croce, G. *et al.* Structural characterization of siliceous spicules from marine sponges. *Biophys. J.* **86**, 526–534 (2004).

Acknowledgements

Beaufour-IPSEN is acknowledged for providing the peptide and European Synchrotron Radiation Facility (ESRF) for allocating beam time (SC801). We are thankful to T. Narayanan for her support during preliminary experiments on the ID02 beamline at the ESRF synchrotron. E. Henry is acknowledged for the capillary picture. This work was supported by the Centre National de la Recherche Scientifique (AC Nanosciences–Nanotechnologies), by a research ministry fellowship (E.P.). Correspondence and requests for materials should be addressed to F.A.
Supplementary Information accompanies this paper on www.nature.com/naturematerials.

Author contributions

F.A. designed the research, with additional contributions from E.D. and M.P. C.V., V.M.-A., M.P. and F.A. initiated the project. E.P., E.D. and A.C. performed TEM experiments. E.P., T.W., A.R. and F.A. performed SAXS experiments. E.P. and A.M. performed Raman experiments. E.P., E.D., M.P. and F.A. analysed data and wrote the paper.

Competing financial interests

The authors declare no competing financial interests.